17th World Conference on Earthquake Engineering, 17WCEE
Sendai, Japan - September 13th to 18th 2020

FLEXURAL PERFORMANCE OF STONE BEAMS STRENGTHENED WITH PREFABRICATED CFRP-REINFORCED STONE PLATES

Y. Ye[1] and Z.X. Guo[2]
[1] *Associate Professor, College of Civil Engineering, e-mail address: qzyeyong@hqu.edu.cn*
[2] *Professor, College of Civil Engineering, e-mail address: guozxcy@hqu.edu.cn*

Abstract

A technique of strengthening the bare stone beams with prefabricated CFRP-reinforced stone plates is proposed and investigated in this research. A thin stone plate embedded with CFRP bars is prefabricated first and then pasted to the tensile surface of stone beams. The prefabricated plate is made of stone which is the same material with that in the strengthened stone beam, so as to maintain the appearance of the traditional structural member. The strengthening effect of this technique is experimentally evaluated herein. Three stone-beam specimens strengthened with such prefabricated plates and one bare stone-beam specimen were tested under four-point bending. The main test parameter considered was the amount of CFRP bars. Test results showed that, the prefabricated plate could shift the failure pattern of a bare stone beam from brittle fracture to a more ductile manner, and significantly increased the load-carrying capacity and deformation capacity of the stone beam. During the loading procedure, good bond behavior was achieved between the prefabricated stone plate and the stone beam, and no end-slip in the CFRP bars was observed, ensuring effective composite actions between the different components. The flexural strength of the strengthened stone beams tends to increase along with the increase of the CFRP reinforcement ratio. This paper could provide reference for the fast strengthening of stone flexural members.

Keywords: Stone beam, Flexural strengthening, CFRP bar, Prefabricated strengthening plate

1. Introduction

In the southeast coastal area of China, a huge number of house buildings constructed with natural stone blocks are still being used by the local residents. It is necessary to point out that, all the structural members in the above house buildings, including the vertical members (masonry walls and columns) and horizontal members (beams and slabs) are made of granite. As known to all that, the tensile strength of natural stone is much lower than the compressive one. Moreover, the stone would experience a brittle fracture once the tensile strength is attained. Thus, there is a potential collapse risk of the stone beams and slabs under overloading or accidental loads.

To improve the brittle failure mode and enhance the mechanical behavior of the flexural members in stone structures, researchers have proposed different strengthening techniques and conducted corresponding investigations so far [1, 2]. Guo et al. [2, 3] proposed a strengthening technique for the stone slabs by using ferrocement mortar, and experimentally investigated the influence of reinforcement ratio and mortar strength on the strengthening effect. Xie et al. [4] investigated the failure mode and flexural strength of stone beams strengthened with a combination of angle steels and polyethylene terephthalate plastic (PET) belts. Liu et al. [5] introduced the strengthening technique of using near-surface mounted (NSM) carbon fiber reinforced polymer (CFRP) bars to stone beams, and conducted experiments to verify the strengthening effect. Based on the research of Liu et al. [5], Ye et al. [6, 7] applied prestress to the NSM CFRPs, and carried out experiments to study the flexural behavior of stone beams and slabs reinforced with prestressed NSM CFRP bars. Zhang et al. [8] and Xie et al. [9] investigated the flexural strength of stone beams strengthened with external prestressed steel wires. Cao et al. [10] and Wu et al. [11] carried out experiments and investigated the failure mode, flexural strength, and deformation capacity of the CFRP-plate strengthened stone beams.

It can be noted from the above review that, the currently available strengthening techniques for stone beams/slabs mainly include applying the ferrocement-mortar, NSM CFRP bars, external CFRP plates or steel wires. These techniques have proved to be effective on improving the flexural strength and deformation capacity of stone beams/slabs. Meanwhile, insufficiency still could be found in these strengthening techniques when used in stone structures, especially in historical buildings. For example, the strengthening technique by using ferrocement-mortar or external CFRP plates/steel wires would spoil the original appearance of the stone members, which is especially important for the protection of historical buildings. The technique by using NSM CFRP bars has relatively little effect on the appearance of the strengthened stone members through, the strengthening process is complex and sometimes difficult to perform on site. Thus, it is a key technical problem to propose a strengthening technique, by using which the flexural behavior of stone beams/slabs can be enhanced with maintaining the original appearance.

Based on the research background, a new strengthening technique for improving the flexural behavior of stone beams is proposed herein. In that technique, an NSM CFRP-reinforced stone plate is fabricated first and then attached to the tensile surface of stone beams with adhesive. The stone plate has a relatively small thickness (weight) and is made of the same material as the stone beam to be strengthened. As a result, this strengthening technique could effectively preserve the appearance of the stone beam and benefit the on-site construction. In order to verify the effectiveness of this strengthening technique, the flexural performance of stone beams strengthened with prefabricated CFRP-reinforced stone plates is experimentally investigated in the current research. This paper could throw light in the further research and engineering application of the proposed strengthening technique for stone flexural members.

2. Test program

2.1 Specimen detail and fabrication process

A total of three strengthened stone-beam specimens (B-2d5-I, B-2d5-II, and B-2d7-I) and one bare stone-beam specimen (B0) were involved in the test campaign. Each stone beam (before strengthening if any) had a cross-section of width (b)× height (h)=150 mm×200 mm with a length (l) of 2000 mm. The width and

length of the prefabricated CFRP-reinforced stone plate were the same as those of the stone beam to be strengthened, while the thickness was 20 mm. Fig. 1 shows the schematic of the cross-sections as well as the groove details. Each prefabricated CFRP-reinforced stone plate had a weight of approximate 17 kg, making it convenient to operate in the strengthening procedure.

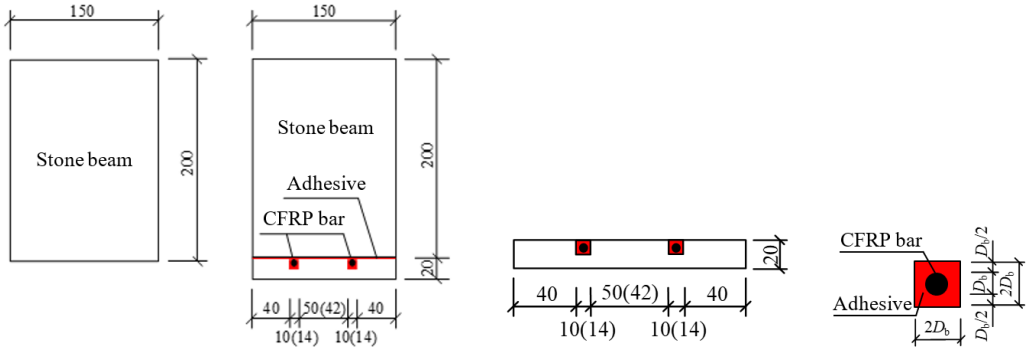

(a) Bare stone beam (b) Strengthened stone beam (c) Prefabricated stone plate (d) Detail of the groove

Fig. 1 – Cross sections of the specimens (all units in mm)

Longitudinal grooves were saw-cut in the stone plate, and then each groove was embedded with one CFRP bar using adhesive. After hardening of the adhesive, the prefabricated CFRP-reinforced stone plate was attached to the tensile surface of the stone beam. In order to minimize the influence on the original appearance of the member to be strengthened, the stone plate had the same texture with the stone beam.

The main test parameter considered in this preliminary research was the CFRP reinforcement ratio. The specimen label and the corresponding parameter are listed in Table 1.

Table 1 – Summary of test information

Specimen ID	D_b (mm)	n	A_b (mm^2)	ρ
B0	-	-	-	-
B-2d5-I	5	2	39.3	0.13%
B-2d5-II	5	2	39.3	0.13%
B-2d7-I	7	2	77.0	0.25%

Note: D_b is the diameter of CFRP bar; n is the number of CFRP bars; A_b is the cross-sectional area of all CFRP bars; ρ is the reinforcement ratio, $\rho=A_b/(bh_0)$, b and h_0 are the width and effective height of the cross section.

The stone used to fabricate the beam specimens was a type of granite, which was mined in Hui'an County of Fujian Province, China. The mechanical properties of the granitic stone were obtained by testing samples, and the average compressive strength, splitting tensile strength, and elastic modulus were 118.2 MPa, 9.1 MPa, and 45 GPa, respectively. The surface of the CFRP bars used in this research was twined with spiral CFRP fiber wires to form the "ribs", so as to increase the bond between the CFRP bar and the adhesive. The tensile strength, elastic modulus, and elongation at fracture of the CFRP bars were tested to be 2853 MPa, 130 GPa, and 2.21%, respectively. The HILTI HIT-RE 500 epoxy adhesive was employed as the bonding agent for both mounting the NSM CFRP bars and bonding the stone plate to the stone beam.

The strengthening process of stone beams with prefabricated NSM CFRP-reinforced stone plates consisted of the following four steps, as shown in Fig. 2.

Step one. Longitudinal grooves were saw-cut on the surface of the stone plate (Fig. 2a). Each groove had a width and depth of twice the diameter of the mounted CFRP bar (D_b). The debris and dust inside the groove were removed by compressed water, after that the stone plate was left to dry at room temperature for 48 hours.

Step two. The CFRP bars were cut to the designed length, and the surface was cleaned with acetone to remove possible dust or oil. The surface of the groove was once again cleaned with compressed air, and then the CFRP bar was embedded into the groove with adhesive (Fig. 2b). The newly fabricated stone plate was left to cure for at least 24 hours.

Step three. The surface, on which side the CFRP bars were mounted, was cleaned with compressed air. Adhesive was laid and flattened on the surface of the stone plate (Fig. 2c).

Step four. The prefabricated NSM CFRP-reinforced stone plate was bonded to the stone beam (Fig. 2d). The strengthened stone beam was left to cure for at least 24 hours without disturbance.

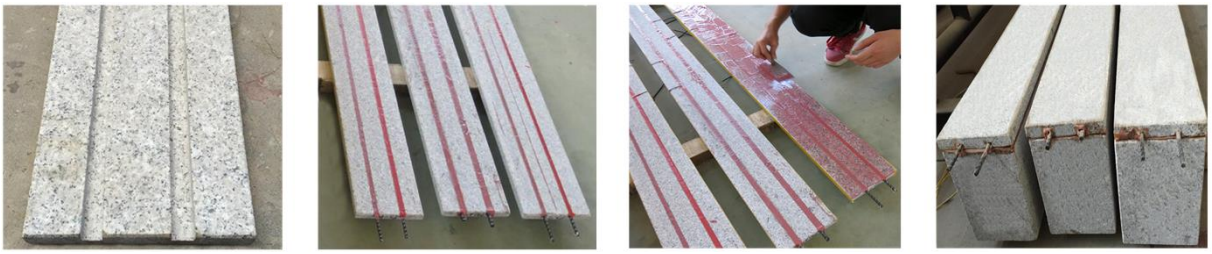

(a) Stone plate with grooves (b) Stone plate with NSM CFRP (c) Adhesive laid on stone plate (d) Strengthened stone beam

Fig. 2 – Construction procedure of strengthened stone beams

2.2 Test setup

A four-point bending test setup was used in the current experiments, as shown in Fig. 3. The center to center distance between the two supports (l_0) was 1,800 mm, and the length of the pure-moment region was 600 mm. The distance between each loading point and the nearest support was 600 mm, resulting in a shear span-to-depth ratio of approximate 3. The load was applied by a vertical hydraulic servo actuator (500 kN capacity) and transmitted to the two loading points (F_1 and F_2) through a rigid steel distribution beam. One fixed hinge-support and one sliding hinge-support were adopted to simulate the simply-supported condition.

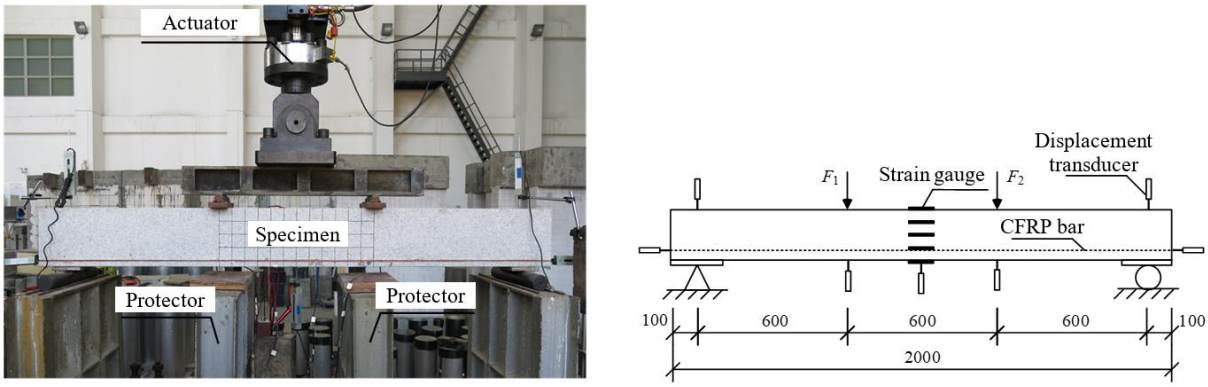

Fig. 3 – Test setup and instrumentation layout

The loading was applied following a force-displacement hybrid control protocol. The load-controlled method was adopted with a load interval of 5 kN until the first crack occurred. After cracking of the stone beam, the control mode was shifted to displacement-controlled mode with a displacement interval of 3 mm until the termination of loading. Between every two adjacent load or displacement intervals, enough time was left for the visual observation. Except for the condition of beam fracture, the loading test was terminated once the mid-span deflection (Δ) attained 12 mm, which was corresponding to Δ/l_0 equal to 1/150.

2.3 Instrumentations

The measurements during testing included the value of the applied vertical load, the deflections of the specimen at both the mid-span and the two loading points, strain distribution along the section height, strain

in the CFRP bar, and slip of the CFRP bar at both ends. Five displacement transducers were arranged at the pure-moment region and the two supports to measure the mid-span deflection. Two displacement transducers were installed at both ends of each CFRP bar to measure the possible slip. Strain gauges were evenly arranged along the section height at the mid-span to measure the strain distribution of the stone beam in the pure-moment region. Strain gauges were also adhered to the surface of CFRP bars in the pure-moment region to measure the strain development of CFRP bars during the loading process. Fig. 3(b) also showed an instrumentation layout of the specimen.

3. Test results and discussion

3.1 Failure mode

When loaded to the cracking load, the bare stone beam (B0) experienced a sudden fracture near the mid-span as expected, see Fig. 4a. The deflection of the bare stone beam before fracture could not be observed by human eyes, exhibiting a typical brittle failure mode. While for the strengthened stone beams, more than one crack appeared and obvious deflection of the specimen was observed. With the increase of the load, new flexural cracks appeared in the pure-moment region of the strengthened stone beam, and the previous cracks developed toward the top edge. The crack distribution for all the four specimens are shown in Fig. 4, where the numbers in the figure indicated the order in which the cracks appeared. When the strengthened stone-beam specimens were loaded to the ultimate deflection of 12 mm, the cracks had extended up to 10-30 mm off the top edge of the stone beam.

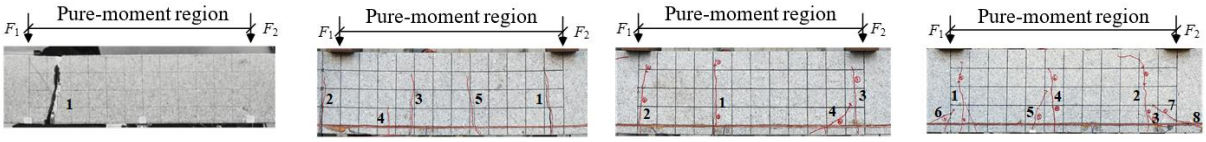

(a) B0 (b) B-2d5-I (c) B-2d5-II (d) B-2d7-I

Fig. 4 – Failure modes and distribution of cracks (Local view)

For the specimens B-2d5-I and B-2d5-II, which had a relatively lower reinforcement ratio, 3-4 flexural cracks and some secondary cracks appeared from the bottom of the pure-moment region and extended upwards. Except for the crack "2" in specimen B-2d5-I, which appeared outside the pure-moment region (Fig. 4b), the other cracks in both specimens B-2d5-I and B-2d5-II were all located in the pure-moment region (Fig. 4b and 4c), and the development direction of the cracks was almost perpendicular to the bottom surface. When the ultimate deflection was reached, the maximum crack width for each strengthened specimen attained 2-3 mm.

Compared with specimens B-2d5-I and B-2d5-II, the specimen with a greater reinforcement ratio B-2d7-I showed a slower crack propagation and a smaller crack width. Meanwhile, secondary cracks were observed near the primary cracks within the pure-moment region, as shown in Fig. 4d.

It is indicated from the above test observations that, increasing the reinforcement ratio of CFRP bars can to some extend suppress the development of flexural cracks. Besides, no slip of the CFRP bar at either end was observed throughout the whole loading procedure, showing favorable bonding performance between the different components.

3.2 Load-deflection responses

The applied vertical load (P) versus mid-span deflection (Δ) curves for all specimens are shown in Fig. 5, where the value of P is the sum of F_1 and F_2 at both loading points. The magnitudes of some feature points in the P-Δ curves are listed in Table 2. It can be seen from Fig. 5 that, the P-Δ curve for the bare stone beam (B0) exhibited a linear increase from the beginning of loading, followed by a sudden drop once the cracking load was reached. While the P-Δ curves for all the strengthened stone beams showed a zigzag shape, with each drop in the curve corresponding to a new crack occurring in the specimen.

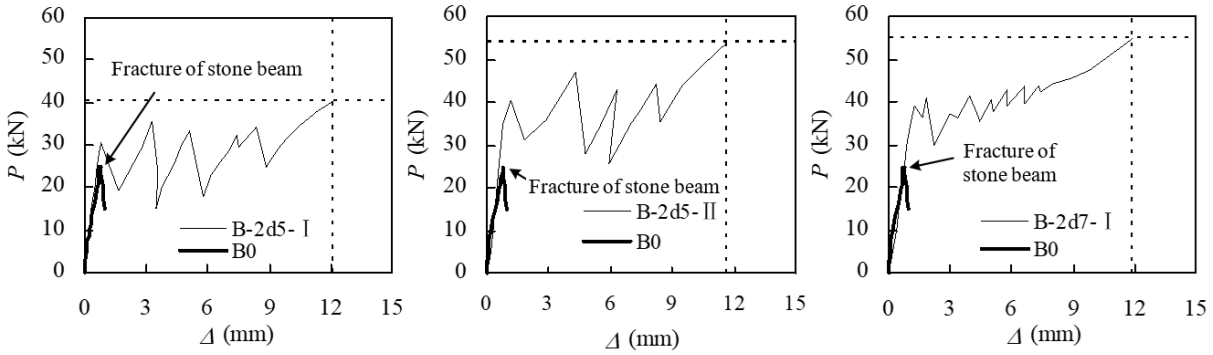

(a) B-2d5-I (b) B-2d5-II (c) B-2d7-I

Fig. 5 – Load-deflection curves

Table 2 – Main experimental results

Specimen ID	P_{cr} (kN)	Δ_{cr} (mm)	P_u (kN)	Δ_u (mm)	P_u/P_{cr}	Δ_u/l_0
B0	24.67	0.75	24.67	0.75	1.000	1/2400
B-2d5-I	30.27	0.78	40.45	12.05	1.336	1/149
B-2d5-II	40.62	1.14	53.74	11.62	1.323	1/155
B-2d7-I	38.97	1.27	54.79	11.97	1.406	1/150

Note: P_{cr} and P_u are the cracking load and ultimate load; Δ_{cr} and Δ_u are the mid-span deflections corresponding to P_{cr} and P_u.

As can be seen in Fig. 5 that, the failure mode of the stone beams strengthened with prefabricated NSM CFRP-reinforced stone plates have been changed from the brittle manner of the bare stone beam to a more ductile manner with remarkable deformation capacity. Thus, the proposed strengthening technique by using prefabricated NSM CFRP-reinforced stone plate could effectively improve the brittle failure mode and enhance the load-bearing capacity of bare stone beams.

It can be noted by comparing Fig. 5(c) with Fig. 5(a) and 5(b) that, with the increase of the CFRP reinforcement ratio, the fluctuation in the *P-Δ* curve decreases when the crack occurs. This is mainly attributed to the fact that, smaller strain increment is needed for a larger amount of CFRP bars to generate the same load-bearing capacity, leading to a smaller crack width and deflection increment.

The ultimate loads (P_u) of specimens B-2d5-I, B-2d5-II, and B-2d7-I were 33.6%, 32.3%, and 40.6% greater than the corresponding cracking loads, respectively, showing good post-cracking strength. It is worth noting that, the maximum mid-span deflection of the test specimens was approximate 12 mm (Δ/l_0=1/150), which was probably not the real ultimate deflection. If the loading continued and the deflection grew beyond Δ=12 mm, the ultimate load might be larger than the one listed in Table 2.

It can be seen from Fig. 5(a) and 5(b) that, the *P-Δ* curve of specimen B-2d5-I [Fig. 5(a)] has a basically similar shape with that of specimen B-2d5-II [Fig. 5(b)]. The value of each peak point in the *P-Δ* curve of B-2d5- II [Fig. 5(b)] is slightly higher than that of specimen B-2d5-I [Fig. 5(a)]. This is mainly due to the dispersion of the stone material, the tensile strength of the stone in B-2d5- II [Fig. 5(b)] is possibly larger than that in B-2d5-I [Fig. 5(a)].

The typical *P-Δ* curve for the stone beams strengthened with prefabricated NSM CFRP-reinforced stone plates is depicted in Fig. 6. Accordingly, the *P-Δ* curve could be divided into three primary stages, as follows:

Elastic stage before cracking (Stage I). In this stage, the load increases almost linearly as the deflection increases until the cracking load (P_{cr}) is reached at a deflection of Δ_{cr}.

Crack propagation stage (Stage II). This stage starts from the formation of the first crack and lasts until the cracks in the pure-moment region fully develop. In this stage, the *P-Δ* curve fluctuates in a zigzag pattern, and each drop of the load corresponds to a newly-formed crack. This is due to the fact that, when the flexural crack occurs from the tensile side of the stone beam, the load originally carried by the stone is transferred to the CFRP bar. The load transfer leads to elongation of the CFRP bar, so the strengthened stone beam experiences the drop of bearing capacity once a new crack appears.

Strain hardening-like stage (Stage III). After full propagation of the cracks in the pure-moment region, the load tends to increase linearly again as the deflection increases, but with a much smaller slope than that in Stage I.

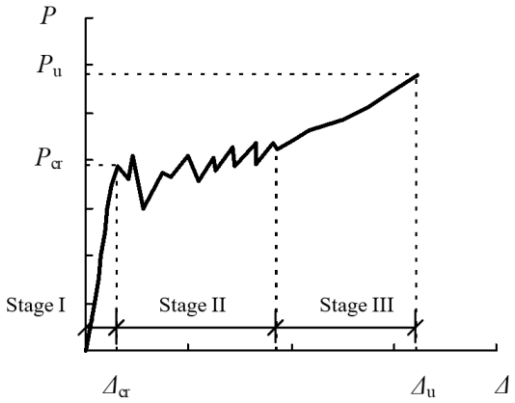

Fig. 6 – Typical load-deflection response for the strengthened stone beams

3.3 Analysis of stone strains

The average strains along the beam height at the mid-span cross section are shown in Fig. 7, where the solid mark and hollow mark in Fig. 7(b) correspond to the strains before cracking and after cracking, respectively. It can be noted that, the stone strains at the bottom edge and top edge were 207 με and 178 με when the cracking of the bare stone beam (B0) occurred, see Fig. 7(a). The strain distribution and development rule of the cross section generally agree with the "plane section remains plane after bending" assumption. The strain in the CFRP bar had a close value to that in the stone at the same location, indicating good bond between the CFRP bar and the stone beam.

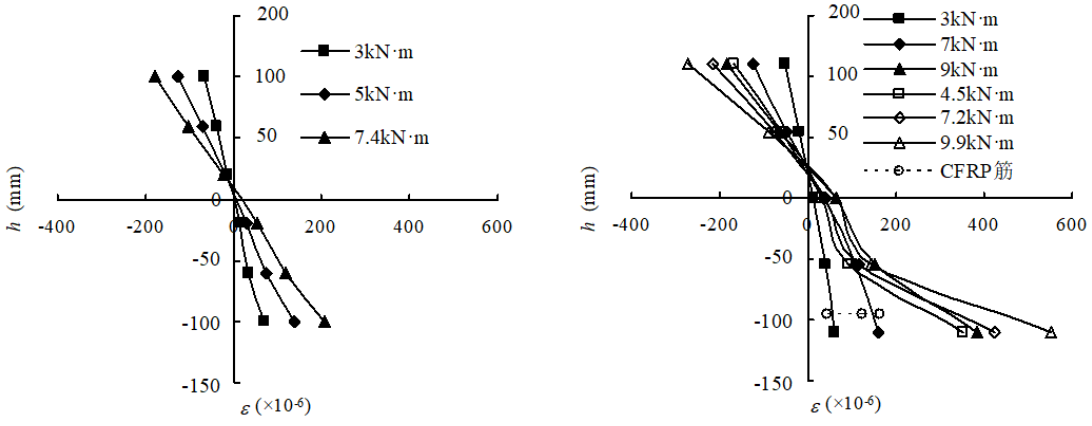

(a) B0 (b) B-2d5-I

Fig. 7 – Strain distribution at mid-span of the stone beams

After cracking of the stone beam occurred, the strain of the stone beam in the compressive region was still approximately linear along the beam height. At the termination of loading, the strain at the top edge of the stone beam had an average value of 772 με. The strain in the CFRP bar experienced obvious increment after the stone in the tensile region failed.

3.4 Strain of CFRP bars

The applied vertical load (P) versus strain of CFRP bars (ε) curves are shown in Fig. 8. Before cracking of the stone beam, the strain of CFRP bars increased linearly with the increase of the load, and the CFRP bars had an average strain of 266 με when the first cracking of stone beam occurred. After that, the tensile force originally carried by the stone was suddenly transmitted to the CFRP bars, leading to rapid increase of CFRP strain near the crack. When a new crack appeared, the strain of the CFRP bar far from the crack might reduce due to the drop of load. Thus, the strain of CFRP bar under the loading point F_2 showed a reduce when the cracking occurred, as shown in Fig. 8(b). After that, the strain of CFRP bar continued to increase again as the load further increased.

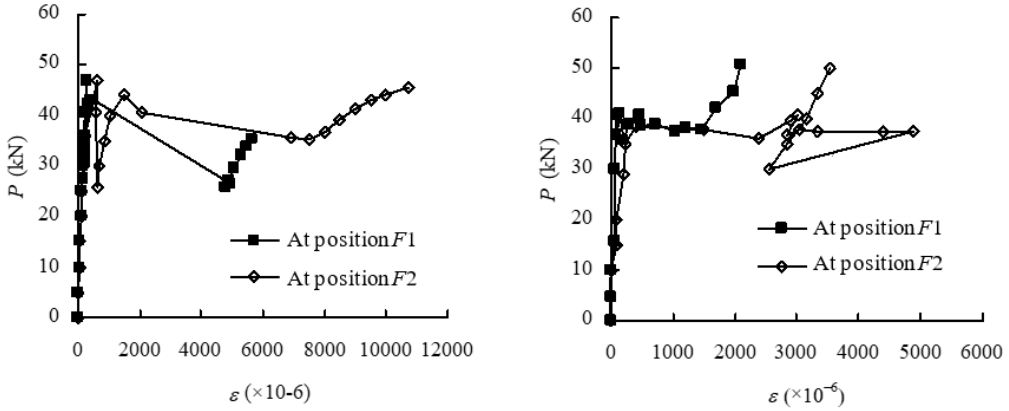

(a) B-2d5-II (b) B-2d7-I

Fig. 8 – Load-CFRP strain curves

The maximum strain of the CFRP bars measured in tests reflects the utilization level of material strength. In the late stage of loading, the maximum measured strains of CFRP bars in specimens B-2d7-I and B-2d5-II were 4873με and 10714με, respectively. It is indicated that, a smaller reinforcement ratio results in a better utilization of the CFRP bars.

4. Conclusions

This paper focuses on the experimental investigation on flexural behavior of stone beams strengthened with prefabricated NSM CFRP-reinforced stone plates, emphasizing the effect of the strengthening technique on improving the brittle failure mode of bare stone beams. Within the parameter range considered herein, the following conclusions could be drawn.

(1) The strengthening technique of using prefabricated NSM CFRP-reinforced stone plates could effectively change the failure mode of bare stone beams from brittle fracture to a more ductile manner with obvious deflection.

(2) Compared with the bare stone beam, the strengthened stone beams have a significantly improved flexural strength and deformation capacity.

(3) During the loading test, satisfactory bond performance between the stone beam and the prefabricated NSM CFRP-reinforced stone plates was achieved. Besides, no end-slip of the CFRP bars occurred, ensuring the composite actions between the reinforcement and the stone beam.

(4) The ultimate flexural strength of specimens B-2d5-I, B-2d5-II, and B-2d7-I was larger than the corresponding cracking moment by 33.6%, 32.3%, and 40.6%, respectively. The strengthening effect tends to increase with the increase of the amount of CFRP reinforcement.

(5) In the future research, prestressing the NSM CFRP bars could be involved in the strengthening technique to further improve the cracking-resistance of the strengthened stone beams and improve the material utilization of the CFRP reinforcement.

5. Acknowledgements

The research reported in the paper is part of the Natural Science Foundation of Fujian Province, P.R. China (Grant No. 2018J01076). The support is greatly appreciated.

6. References

[1] Guo ZX, Huang QX, Chai ZL, Liu Y (2009): Study and prospect of disaster prevention technology of stone masonry structures. *Earthquake Resistant Engineering and Retrofitting*, 31(6), 47-57. (in Chinese)

[2] Guo ZX, Wang L, Chai ZL, Ye Y, Shahrooz BM (2017): Flexural behavior of stone slabs strengthened with reinforced mortar. *Construction and Building Materials*, 18(4), 158-167.

[3] Guo ZX, Wang L, Chai, ZL, Liu, Y, Li G, Yi TH (2011): Experimental study on flexural behavior of stone slabs strengthened with ferrocement mortar. *Journal of Building Structure*, 32(3), 69-74. (in Chinese)

[4] Xie J, Wu XM, Xu FQ (2016): Experimental study on the flexural behavior of stone beams strengthened with a combination of angle steels and PET belts. *Materials and Structures*, 49(3), 1013-1024.

[5] Liu Y, Guo, ZX, Liu BC, Ye Y (2011): Experimental study on flexural behavior of NSM CFRP-stone composite beams. *Journal of Building Structures*, 32(3), 75-81. (in Chinese)

[6] Ye Y, Guo ZX, Chai ZL (2014): Flexural behavior of stone slabs reinforced with prestressed NSM CFRP bars. *Journal of Composites for Construction-ASCE*, 18(4), 04014004.

[7] Ye Y, Guo ZX, Liu Y, Wang L (2014): Flexural behavior of stone beams reinforced with prestressed NSM CFRP bars. *Construction and Building Materials*, 54, 466-476.

[8] Zhang XH, Lin BG, Jiao HZ, Hou W (2011): Experimental study on flexural resistance of prestressed large-span stone beam. *Journal of Xi'an University of Architecture & Technology (Natural Science Edition)*, 43(2), 172-177. (in Chinese)

[9] Xie J, Li R, Wu XM, Xu FQ (2015): Experimental study on flexural behaviors of stone beams strengthened with external prestressing. *Building Structure*, 45(16), 96-100. (in Chinese)

[10] Cao SW, Zhao D, Chen P (2010): Test research on stony beams strengthened by CFRP. *Building Structure*, 40(5), 53-54. (in Chinese)

[11] Wu XM, Xie J, Xu FQ, Qi W (2015): Experimental study on flexural behaviors of stone beams strengthened by CFRP. *Engineering Mechanics*, 32(Suppl), 215-220. (in Chinese)

